H. hepaticus-induced liver tumor promotion is associated with increased serum bile acid and a persistent microbial-induced immune response

Citation: Garcia, A. et al. "Helicobacter hepaticus-Induced Liver Tumor Promotion Is Associated with Increased Serum Bile Acid and a Persistent Microbial-Induced Immune Response." Cancer Research 71.7 (2011): 2529–2540.

As Published: http://dx.doi.org/10.1158/0008-5472.CAN-10-1975

Publisher: American Association for Cancer Research

Persistent URL: http://hdl.handle.net/1721.1/75430

Version: Author's final manuscript: final author's manuscript post peer review, without publisher's formatting or copy editing

Published in final edited form as:
Cancer Res. 2011 April 1; 71(7): 2529–2540. doi:10.1158/0008-5472.CAN-10-1975.

H. hepaticus-induced liver tumor promotion is associated with increased serum bile acid and a persistent microbial-induced immune response

Alexis García[1], **Yu Zeng**[2], **Sureshkumar Muthupalani**[1], **Zhongming Ge**[1], **Amanda Potter**[1], **Melissa W. Mobley**[1], **Chakib Boussahmain**[1], **Yan Feng**[1], **John S. Wishnok**[2], and **James G. Fox**[1,2]

[1] Division of Comparative Medicine, Massachusetts Institute of Technology, Cambridge MA

[2] Department of Biological Engineering, Massachusetts Institute of Technology, Cambridge MA

Abstract

Chronic microbial infection influence cancer progression but the mechanisms that link them remain unclear. Constitutive androstane receptor (CAR) is a nuclear receptor that regulates enzymes involved in endobiotic and xenobiotic metabolism. CAR activation is a mechanism of xenobiotic tumor promotion, however, the effects of chronic microbial infection on tumor promotion have not been studied in the context of CAR function. Here we report that CAR limits the effects of chronic infection-associated progression of liver cancer. CAR knockout (KO) and wild-type (WT) male mice were treated or not with the tumor initiator diethylnitrosamine (DEN) at 5 weeks of age and then orally inoculated with *Helicobacter hepaticus* (Hh) or sterile media at 8 weeks of age. At 50 weeks postinoculation mice were euthanized for histopathological, microbiological, molecular, and metabolomic analyses. Hh infection induced comparable hepatitis in WT and KO mice with or without DEN that correlated with significant upregulation of *Tnfα* and toll receptor *Tlr2*. Notably, DEN-treated Hh-infected KO mice exhibited increased numbers of liver lobes with dysplasia and neoplasia, as well as increased multiplicity of neoplasia, relative to similarly treated WT mice. Enhanced tumor promotion was associated with decreased hepatic expression of P450 enzymes *Cyp2b10* and *Cyp3a11*, increased expression of *Camp*, and increased serum concentrations of chenodeoxycholic acid. Together, our findings suggest that liver tumor promotion is enhanced by an impaired metabolic detoxification of endobiotics and a persistent microbial-induced immune response.

Keywords

Nuclear receptor; *Helicobacter hepaticus*; innate immunity; bile acid; liver cancer

Introduction

Nuclear receptors are transcription factors that link gastrointestinal microflora, innate immunity, and metabolism through toll-like receptors (TLR's) (1). The NR1 subfamily of nuclear receptors consists of vitamin D receptor (VDR/NR1I1), pregnane X receptor (PXR/NR1I2), and constitutive androstane receptor (CAR/NR1I3); each of which is capable of inducing the expression of broad-specificity hepatic and intestinal phase I enzymes (CYP2C9 and CYP3A4) that play major roles in metabolic detoxification of xenobiotics and endobiotics such as bile acids (2). VDR, PXR, and CAR perform overlapping functions in altering bile acid metabolism and elimination. Bile acids in turn may exert adverse effects including tumor promotion (3-5).

Postulated mechanisms of liver tumor promotion include chronic cytotoxicity and sustained activation of nuclear receptors. Chronic CAR activation using phenobarbital, a prototype rodent liver tumor promoter, leads to hepatomegaly and hepatocellular carcinoma in mice (6,7). *H. hepaticus* (Hh) is the prototype carcinogenic bacterium of mice and experimental infection has been used as a model of microbial tumor promotion in the liver, colon, and mammary glands (8-11). Various helicobacter infection models have also suggested a link between disrupted metabolism and immunity in disease pathogenesis. For example, selected enterohepatic *Helicobacter* species, but not *H. pylori*, play a role in the pathophysiology of cholesterol gallstone formation in C57L/J mice fed a lithogenic diet (12). Progression to hepatocellular carcinoma in *H. hepaticus*-infected F1 hybrid male mice is linked to hepatic expression of lipogenic genes and immune function associated networks (13). In the present study, we investigated the role of nuclear receptor function and chronic enterohepatic *Helicobacter* infection on hepatic cancer progression, and discovered a link between impaired metabolic detoxification, bile acids, and microbial-induced immune response in carcinogenesis.

Materials and Methods

Mice

CAR knockout (KO, C3H/HeNCrl background) mice were obtained from Integrated Laboratory Systems, Inc. (Research Triangle Park, NC), embryo transfer re-derived and housed in *Helicobacter*-free facilities. The original C57BL/6X129 background of this CAR KO mice have been changed to a liver-tumor susceptible mouse strain by repeated backcrossing to C3H/HeNCrlBR (7). *Helicobacter*-free CAR wild-type (WT, C3H/HeNCrl) mice were obtained from Charles River Laboratories (Wilmington, MA). All mice were fed a commercial rodent diet (Prolab® RMH 3000, LabDiet®, St. Louis, MO) ad libitum and housed in Association for Assessment and Accreditation of Laboratory Animal Care International-approved facilities. All experiments were approved by the Massachusetts Institute of Technology Institutional Animal Care and Use Committee.

Experimental Design

Groups consisting of $CAR^{-/-}$ (KO) and $CAR^{+/+}$ (WT) mice are described in Table 1. Briefly, a group of 43 KO male mice and a group of 43 WT male mice were each divided into two groups. One group of each genotype (22 KO and 23 WT) under isoflurane anesthesia was given a single intraperitoneal injection of the carcinogen (as tumor initiator) diethylnitrosamine [(DEN) 45 mg/kg] (ISOPAC®; N0258, Sigma-Aldrich Co., St. Louis, MO) at 5 weeks of age. The other group of mice (21 KO and 20 WT) did not receive carcinogen. The mice were subsequently subdivided into four groups (two KO and two WT groups) and orally inoculated with either ~10^9 CFU's of Hh (ATCC 51449) (as a tumor promoter) or sterile media at 8 weeks of age for three doses received on different days. At approximately 30 weeks postinoculation (pi) 3 mice in each group of WT+DEN and WT +DEN+Hh were euthanized and complete necropsies were performed for tumor assessment. At the end of the study (~50 weeks pi) seventy mice were euthanized and complete necropsies were performed. Body weight, liver weight, and total number of gross liver tumors were recorded.

Histopathological evaluation

Samples from all the liver lobes were collected, fixed in 10% neutral buffered formalin, embedded in paraffin, sectioned at 5 μm, and stained with hematoxylin and eosin. Special care was taken to identify and include all grossly visible tumors in the representative histological sections from each liver lobe. Histopathological evaluation was performed by a board-certified veterinary pathologist blinded to the identity of the samples. Liver sections

were scored as previously described with minor modifications (14,15). Briefly, hepatic lobular, portal and interface inflammation was graded on a scale of 0-4 and the number of lobes with ≥ 5 inflammatory foci was enumerated. The cumulative scores from all the above mentioned criteria were represented as a hepatitis index (HI). Hepatitis was defined as HI score of ≥ 4 (15). Additionally, all liver lobes were assessed for the type and total numbers of preneoplastic and neoplastic foci as described earlier and adapted from the National Toxicology Program (14). Various preneoplastic tinctorial and cytological alterations, also termed as foci of altered hepatocytes (FAH), were classified and counted as one of the following: eosinophilic cell foci, basophilic cell foci, clear cell/vacuolated cell foci, mixed cell foci (combination of basophilic and clear/vacuolated cell foci), large foci of cellular alteration (LFCA), and dysplastic foci (with or without cytoplasmic tinctorial alterations). Hepatocellular adenoma (HCA) and hepatocellular carcinoma (HCC) and biliary neoplasms were also enumerated in each individual liver lobe. For each animal, the number of liver lobes with dysplasia (FAH/LFCA) and/or neoplasia (HCA/HCC) was also determined. Images were obtained using an Olympus BX41 microscope and DP25 digital camera and image acquisition software.

Microbiological analyses

DNA was extracted from tissue (liver and cecum) by using the HighPure PCR Template Preparation Kit (Roche Diagnostics GnbH, Mannaheim, Germany). Hh real-time quantitative PCR on cecum and liver DNA was performed as previously described (16).

Gene expression analyses

Total RNA from liver samples stored at -80°C was extracted using TRIzol reagent. For quantification of mRNA, 5 μg of total RNA from each liver sample was converted into cDNA with a High Capacity cDNA Archive Kit (Applied Biosystems, Foster City, CA). The cDNA levels of pregnane X receptor (PXR/*Nr1i2*), farsenoid X receptor (FXR/*Nr1h4*), vitamin D receptor (*Vdr/Nr1i1*), toll-like receptor 2 (*Tlr2*), p65 (*Rela*), tumor necrosis factor (*Tnfα*), interleukin 6 (*Il6*), cathelicidin antimicrobial peptide (*Camp*), cytochrome P450, family 3, subfamily a, polypeptide 11 (*Cyp3a11*), cytochrome P450, family 2, subfamily b, polypeptide 10 (*Cyp2b10*), hepatocyte growth factor (*Hgf*), and catenin, beta 1 (*Ctnnb1*) were determined by quantitative PCR using commercially available primers and probes (Applied Biosystems). Gene expression was normalized relative to the cDNA levels of glyceraldehyde-3-phosphate dehydrogenase (Gapdh). Most reactions were performed in duplicate containing a total volume of 20 μl including 5 μl of cDNA, 1 μl of primer-probe solution, 10 μl of Master Mix, and 4 μl of RNAase-free water. The relative expression of mRNA was calculated as described in the TaqMan protocol. The mRNA levels were expressed as the fold-change relative to WT mice (uninfected and without DEN).

Cathelicidin immunohistochemistry

Five randomly selected livers (at least four sections per liver) from each relevant group (WT, WT+DEN, WT+DEN+Hh, KO, KO+DEN, KO+DEN+Hh) were used for evaluation of cathelicidin immunoreactivity. Immunohistochemistry was performed on formalin-fixed paraffin-embedded livers sectioned at a thickness of 4 μm, deparaffinized, followed by antigen retrieval by steaming. The sections were incubated for 10 min each at room temperature with avidin and followed by biotin for blocking non-specific binding sites. Subsequently, the sections were incubated overnight (12-15 hrs) at 4°C with a rabbit polyclonal antibody to mouse cathelicidin (ab74868, Abcam, Cambridge, MA) at a dilution of 1:1200. After thorough washing in buffer, the sections were incubated with a biotinylated polyclonal goat anti-rabbit IgG antibody (Dako North America Inc., Carpinteria, CA) at a dilution of 1:1000 for 20 min. After washing in PBS buffer, the sections were treated with 3% H_2O_2 for 10 min, followed by incubation with streptavidin-HRP for 20 min, washed

again in PBS buffer, and finally incubated with diaminobenzidine, washed and counterstained with hematoxylin and mounted. Cathelicidin immunoreactivity in the liver was semi-quantitatively graded on a scale of 0-3 i.e., none (0), mild (1), moderate (2), and marked (3), separately under 3 distinct categories namely, hepatocytes, inflammatory cells/ kupffer cells and biliary epithelium. The cumulative scores from all the three groups of cells in the liver was defined as Cathelicidin Labeling Index (LI).

Quantitative profiling of serum bile acids by liquid chromatography tandem mass spectrometry (LC-MS/MS)—Lithocholic acid (LCA), cholic acid (CA), taurocholic acid (TCA) sodium salt hydrate, ursodeoxycholic acid (UDCA), and chenodeoxycholic acid (CDCA) were purchased from Sigma-Aldrich. 5ß-cholanic acid-3-one (keto-LCA) and 5ß-cholanic acid-3α-olacetate (LCA-acetate) were purchased from Steraloids, Inc. (Newport, RI). The internal standard, cholic 2,2,4,4-d_4 acid (CA-d_4), was purchased from C/D/N Isotopes, Inc. (Pointe-Claire, Quebec, Canada).

Mouse serum samples were stored at -20°C or -80°C prior to analyses. Samples were thawed, vortexed, and 25 μl aliquots were inoculated with CA-d4 and then with 1 ml of cold acetonitrile to precipitate the serum proteins. Following centrifugation for 15 minutes at ~15,000 g, the supernatants were collected individually and dried in a Speed Vac. The residues were dissolved in 50 μl of water and centrifugation was repeated. Clear supernatants (40 μl) were transferred to autosampler-vial inserts for LC-MS/MS analysis.

Detection and quantification of the bile acids were performed on an ESI-tandem-quadrupole mass spectrometer (Agilent Technologies 6430). The HPLC system consisted of an Agilent 1200 binary pumping system and an Eclipse XDB-C18 column (1.0*50 mm i.d. 3.5 μm, Agilent) operated at a flow rate of 10 μl/min. Injection volume was 3 μl. Separations were achieved with the following gradient: 100% buffer A from 0 to 16 min, then 100% buffer B from 18 to 26 min. Buffers A and B were 90% and 100% MEOH, respectively, and both had 10 mM ammonium acetate and 0.1% formic acid. The HPLC eluents from 0 to 2 minutes were directed to waste to avoid salt contamination. The mass spectrometer was operated in negative electrospray ionization mode with the following parameters: electrospray voltage: 2000V; drying gas: 350°C at 8 l/min; fragmentor: 90V; collision energy: 15V; nebulizer pressure: 40 psi; scan time per transition, 200 ms. The collision gas pressure in this instrument is set internally by the firmware.

Multiple Reaction Monitoring (MRM) transitions for the various bile acids were as follows: TCA (*m/z* 514.4→514.4), CA (*m/z* 453.3→407.2), UDCA (*m/z* 437.3→391.1), CDCA (*m/z* 437.3→391.1), CA-d4 (*m/z* 411.2→411.2), LCA (*m/z* 421.4→375.4), keto-LCA (*m/z* 373.3→373.3) and LCA-acetate (*m/z* 417.3→417.3).

The calibration curves (6 points) were constructed over the range of 5 – 500 ng/ml using serum from a WT mouse (uninfected and without DEN), with CA-d4 as the internal standard.

Statistical analyses—Enhanced hepatic tumor promotion was defined as the comparison between WT and KO mice that received DEN and were infected with Hh (WT+DEN+Hh and KO+DEN+Hh, respectively). Multiplicity of preneoplasia or neoplasia was defined as the average number of microscopic preneoplastic (FAH and LFCA combined) or neoplastic (HCA and HCC combined) liver lesions per mouse (17). Results were expressed as mean ± SEM (for histopathology, immunohistochemistry, colonization, and serum bile acid data) or mean ± SD (for gene expression data). Comparisons were performed using 2-tailed Mann-Whitney tests and/or Student's t-tests. A P value of ≤ 0.05 was considered significant.

Results

Increased hepatitis index (HI) is noted after Hh infection

At ~30 weeks pi the HI score in WT+DEN mice was 0 whereas the HI score in WT+DEN +Hh mice ranged from 2.5 to 8.5. One or two mice per group developed hepatic adenomas.

Increased liver tumor promotion during CAR deficiency and chronic Hh infection

Grossly, at the end of the study (~50 weeks pi), the liver to body weight ratio (%) of KO +DEN+Hh mice appeared increased relative to that of WT+DEN+Hh mice (P=0.07) (Supplementary Fig. S1). The number of grossly visible liver tumors in KO+DEN+Hh mice was significantly higher than that of WT+DEN+Hh mice (6.17 ± 0.76 vs. 2.75 ± 0.56, P<0.004). The number of grossly visible liver tumors was not significantly different when comparing WT+DEN and WT+DEN+Hh; however, a significantly increased number of liver tumors was observed in KO+DEN+Hh mice relative to KO+DEN mice (6.17 ± 0.76 vs. 3.17 ± 1.38, P=0.05) (Supplementary Fig. S2).

Histologically, KO+DEN+Hh mice exhibited morphological lesions suggestive of tumor progression including FAH (basophilic, eosinophilic, and/or clear cell, LFCA), HCA, and HCC (schematic representation, Fig. 1A). The cells within the adenomas and carcinomas frequently exhibited a mixture of one or more of the tinctorial cytological alterations as seen in FAH. In Hh-infected livers, large non-discrete ill-defined areas of increased hepatocellular atypia with cytoplasmic tinctorial alterations and visible mitotic activity indicative of dysplastic changes were also observed with or without HCC in the affected lobe (Fig. 1A). In Hh-infected animals, variable inflammation was present either within or surrounding the dysplastic and neoplastic nodular foci (Fig. 1A). KO+DEN+Hh mice exhibited a significantly increased number of liver lobes with dysplasia and neoplasia compared to WT+DEN+Hh mice (3.58 ± 0.15 vs. 2.25 ± 0.25, P<0.0001). WT+DEN+Hh mice also demonstrated a significantly increased number of dysplastic and neoplastic liver lobes compared to WT mice (2.25 ± 0.25 vs. 0.89 ± 0.35, P<0.008). The number of dysplastic and neoplastic liver lobes was not significantly different when comparing WT +DEN vs. WT+DEN+Hh or KO+DEN vs. KO+DEN+Hh (Fig. 1B). The multiplicity of neoplasia including HCA and HCC in KO+DEN+Hh mice was also significantly higher than that of WT+DEN+Hh mice (5.08 ± .53 vs. 2.63 ± .60, P<0.007) which also exhibited a significantly increased multiplicity of liver tumors compared to WT mice (2.63 ± .60 vs. 1.00 ± .37, P<0.03). Consistent with this increase in tumors, the multiplicity of preneoplasia in WT+DEN+Hh was significantly increased relative to WT mice (2 ± .63 vs. .22 ± .15, P<0.01). No significant differences in multiplicity of preneoplasia and neoplasia were observed when comparing WT+DEN vs. WT+DEN+Hh or KO+DEN vs. KO+DEN+Hh (Fig. 1C).

All Hh-infected mice developed significantly increased HI scores relative to uninfected WT mice (P<0.05) (Fig. 1A). Comparable HI scores were observed in all groups of Hh-infected mice and there was no significant difference between KO+DEN+Hh and WT+DEN+Hh mice (4.71 ± .93 vs. 4.75 ± 1.21, P=1.0) (Fig. 1D).

Decreased Hh colonization is observed during liver tumor promotion

A trend towards lower numbers of Hh was observed in the liver of KO+DEN+Hh mice compared to WT+DEN+Hh mice (1.95×10^5 vs. 5.83×10^5, P=0.07) and KO+Hh mice (1.95×10^5 vs. 6.78×10^5, P=0.07). No significant difference was observed between WT+Hh and WT+DEN+Hh (1.08×10^6 vs. 5.83×10^5; P=0.27) (Fig. 2A). In the cecum, KO+DEN+Hh and WT+DEN+Hh mice had comparable numbers of Hh (3.24×10^6 vs. 2.07×10^6, P=0.21). However, significantly lower numbers of Hh were detected in WT+DEN+Hh and KO+DEN

+Hh mice when compared to WT+Hh (2.07×10^6 vs. 9.59×10^6, P<0.003) and KO+Hh (3.24×10^6 vs. 7.78×10^6, P<0.01) mice, respectively (Fig. 2B).

No significant differences in Hh colonization were observed in the cecum or liver of WT +Hh mice relative to KO+Hh mice (cecum: 9.59×10^6 vs. 7.78×10^6, respectively, P=0.50; liver: 1.08×10^6 vs. 6.78×10^5, respectively, P=0.40).

Gene expression analyses

Transcription of genes significantly modulated in KO+DEN+Hh relative to WT+DEN+Hh

Hepatic downregulation of *Cyp2b10* and *Cyp3a11*—*Cyp2b10*** was significantly downregulated in WT+Hh (P<0.02) and WT+DEN+Hh (P<0.002) and in all groups of KO mice [KO (P<0.0001), KO+Hh (P<0.0001), KO+DEN (P<0.0001), KO+DEN+Hh (P<0.0001)] relative to WT mice. Furthermore, *Cyp2b10* was significantly downregulated in KO+DEN+Hh mice compared to WT+DEN+Hh mice (P<0.0001) (Fig. 3A).

Similarly, *Cyp3a11* was significantly downregulated in most groups of KO mice [KO (P<0.02), KO+DEN (P=0.05), KO+DEN+Hh (P<0.006)] relative to WT mice. *Cyp3a11* was significantly downregulated in KO+DEN+Hh mice compared to WT+DEN+Hh mice (P<0.01) (Fig. 3B).

Hepatic upregulation of *Camp*—*Camp*** was significantly upregulated in KO+Hh mice (P<0.04) and KO+DEN+Hh mice (P<0.0009) relative to WT mice. KO+DEN+Hh mice showed significant hepatic upregulation of *Camp* compared to WT+DEN+Hh mice (P<0.03) (Fig. 3C).

Transcription of genes with comparable modulation in KO+DEN+Hh relative to WT+DEN +Hh

Comparable hepatic upregulation of *Tlr2* and *Tnfα* during chronic Hh infection —Significantly increased hepatic mRNA levels of *Tlr2* and *Tnfα* were detected in all Hh-infected groups [WT+Hh (P<0.002 and P<0.02, respectively; WT+DEN+Hh (P<0.02 and P<0.04, respectively); KO+Hh (P<0.007 and P<0.01, respectively); KO+DEN+Hh (P<0.0001 and P<0.001, respectively)] relative to uninfected WT mice. KO+DEN+Hh and WT+DEN+Hh mice showed comparable hepatic upregulation of *Tlr2* and *Tnfα* (P>0.05) (Fig. 3D-E). These results correlated well with comparable hepatitis indices observed in all Hh-infected groups.

Transcription of genes significantly upregulated in KO+DEN+Hh relative to WT

Hepatic upregulation of *Vdr* and FXR—In WT mice, *Vdr* expression was significantly upregulated by infection alone (P<0.0007), DEN alone (P<0.01), and the combination of DEN+Hh (P<0.004). *Vdr* expression was also significantly upregulated in KO mice relative to WT mice (P<0.005). The expression of *Vdr* in KO+Hh and KO+DEN+Hh mice was significantly upregulated relative to WT mice (P<0.005 and P<0.0001, respectively) (Fig. 4A).

The expression of FXR in WT mice was significantly upregulated by DEN alone (P<0.05) and the combination of DEN+Hh (P<0.0002). Significant upregulation of FXR was detected in KO mice relative to WT mice (P<0.001). Neither KO+Hh or KO+DEN mice exhibited significant upregulation of FXR relative to WT mice; however, the combination of DEN+Hh in KO mice significantly upregulated FXR relative to WT mice (P<0.03) (Fig. 4B).

Infection alone significantly upregulated hepatic PXR expression in WT mice (P<0.02) (Supplementary Fig. S3).

Hepatic upregulation of *Rela* and *Il6*—The expression of *Rela* in WT mice was significantly upregulated by infection alone (P<0.02), DEN alone (P<0.007), and the combination of DEN+Hh (P<0.002). Significant upregulation of *Rela* was detected in KO mice relative to WT mice (P<0.01). Neither KO+Hh or KO+DEN mice exhibited significant upregulation of *Rela* relative to WT mice; however, the combination of DEN+Hh in KO mice significantly upregulated *Rela* relative to WT mice (P<0.0001) (Fig. 4C).

In WT mice, *Il6* expression was significantly upregulated by infection alone (P<0.003), DEN alone (P<0.01), and the combination of DEN+Hh (P<0.002). *Il6* expression was also significantly upregulated in KO mice relative to WT mice (P<0.004). The expression of *Il6* in KO+Hh and KO+DEN+Hh mice was significantly upregulated relative to WT mice (P<0.02 and P<0.0007, respectively) (Fig. 4D).

Hepatic upregulation of beta-catenin—Hepatic *Ctnnb1* expression was significantly upregulated in KO+DEN+Hh mice relative WT mice (P<0.006) (Supplementary Fig. S4).

No significant differences were noted on *Hgf* expression in the different groups of mice (Supplementary Fig. S5).

Cathelicidin immunoreactivity in the liver of KO mice is significantly correlated with chronic Hh infection

Uninfected WT (Fig. 5A) and KO mice (not shown) had no to sparse cathelicidin immunoreactivity in the cytoplasm of hepatocytes and biliary epithelium and mild to moderate positive staining in Kupffer cells. In infected livers, cathelicidin was highly expressed in the cytoplasm of inflammatory cells; primarily neutrophils and macrophages (Fig. 5B-C). Variable increased cytoplasmic positivity above background levels was also observed in hepatocytes of infected livers of WT and KO mice. Also, Kupffer cells of both infected and uninfected livers had recognizable cytoplasmic cathelicidin staining.

A semi-quantitative analysis of immunohistochemical data from different groups, revealed a significantly higher cathelicidin LI (P<0.01) in the liver of KO+DEN+Hh mice compared to liver from uninfected WT and KO mice (KO, KO+DEN) (Fig. 5D).

Increased circulating concentration of CDCA in KO mice is associated with chronic Hh infection during liver tumor promotion—The serum concentration (nmol/L) of CDCA was significantly increased in KO+DEN+Hh mice compared to WT +DEN+Hh mice (70.24 ± 17.60 vs. 16.33 ± 4.552, P<0.02). The serum CDCA concentration was also significantly increased in KO+DEN+Hh mice relative to WT mice (70.24 ± 17.60 vs. 10.78 ± 5.012, P<0.01) (Fig 6).

The serum concentration of TCA was significantly increased in WT+DEN+Hh mice (30390 ± 13970, P<0.05) and KO+DEN+Hh mice (32530 ± 9212, P<0.01) relative to WT mice (921.9 ± 804.7) (data not shown). Infection alone (WT+Hh, 14.82 ± 1.435, P<0.02) significantly increased serum LCA concentration in WT mice (8.749 ± 1.901) (data not shown).

The serum concentration of other measured bile acids including keto-LCA, LCA-acetate, CA, and UDCA was not significantly different in the other groups of mice relative to WT mice and no other differences were noted between WT+DEN+Hh and KO+DEN+Hh mice.

Discussion

Chronic CAR activation by the xenobiotic phenobarbital, a prototype tumor promoter of mice, has been recognized as a mechanism of tumor promotion (6,7). Our study, using a well-established model of tumor initiation and promotion in *Helicobacter*-free CAR deficient mice, demonstrates that CAR deficiency potentiates experimental microbially-driven tumor promotion initiated by DEN. Our findings of increased liver tumorigenicity coupled with decreased *Cyp2b10* and *Cyp3a11* expression in KO+DEN+Hh mice relative to WT+DEN+Hh mice support a protective role of CAR, *Cyp2b10*, and *Cyp3a11* from endobiotics during chronic Hh infection and tumor promotion. CAR activators including phenobarbital and TCPOBOP protect the liver against bile acid-induced toxicity through a mechanism involving changes in bile acid composition (18). *Cyp2b10* and *Cyp3a11* encode phase I hydroxylation enzymes important for detoxification of hepatic bile acids and biliary compounds (19). Hydroxylation renders bile acids more hydrophilic and consequently less toxic (19). In addition, our findings suggest that CAR may be important for basal expression of *Cyp3a11* as suggested in experiments using androstenol, a CAR inverse agonist (20). We propose a mechanism by which a chronic enterohepatic microbial infection promotes liver tumors during pathophysiological states. This process involves metabolic deficiencies in nuclear receptors and their modulating effects on enzymes involved in metabolic detoxification. Our findings are, in principle, broadly consistent with previous studies that demonstrated that a deficiency of FXR, a central regulator of bile acid metabolism, predisposed mice to liver and intestinal tumors (21-24).

We hypothesized that changes in bile acid homeostasis played a role in tumor promotion during chronic infection and CAR deficiency in mice. The serum concentration of CDCA was elevated in Hh-infected KO mice during liver tumor development. These results are consistent with the tumor promoting effects observed with CDCA in the colon and liver of rats and in the duodenum of a mouse model of familial adenomatous polyposis (25-27). CDCA has been found to be elevated in the serum of human patients with cholangiocarcinoma and hepatocellular carcinoma and could be used as a biomarker for these conditions (28). CDCA and LCA induced transcription factor Snail expression and repressed E-cadherin in HCC and cholangiocarcinoma cell lines (29). During CAR activation and hepatoprotection in mice, the concentration of CDCA in the liver may be decreased (18). Although a mechanism of tumor promotion elicited by increased concentration of CDCA has not been elucidated, it is possible that increased synthesis and/or decreased catabolism of CDCA may account for these findings. Deficient expression of cytochrome P450 enzymes such as CYP3A4 may play a role in decreased biotransformation of CDCA (30). In addition, changes in the gastrointestinal microflora can impact bile acid metabolism through a decrease in 7α-dehydroxylating bacteria which convert CDCA to LCA and/or an increase in those bacterial species which convert UDCA to CDCA (31,5). For example, Hh infection in mice can influence the intestinal colonization dynamics of Altered Schaedler Flora, a set of eight anaerobic bacterial species commonly used to establish normal physiological function in the mouse gastrointestinal tract and provide overall diversity of the microbial community (32,33). It is therefore possible that perturbing the colonization dynamics due to Hh infection could have influenced CDCA levels in this study.

Hepatic upregulation of *Vdr* in KO and KO+DEN+Hh mice relative to WT mice suggested that this nuclear receptor played a role in bile acid detoxification and tumor promotion. Upregulation of *VDR* has been observed in livers of human patients with hepatocellular carcinoma (34). Previous studies demonstrated that VDR was activated by the toxic secondary bile acid LCA which induced its own detoxification through VDR-mediated expression of CYP3A (35). This finding led to a hypothesis to explain the effect of VDR and

bile acids on colon tumor promotion and why vitamin D, which also activates VDR, is protective against development of colon cancer (35). It is postulated that inadequate LCA metabolism by VDR target enzymes in conditions such as sustained high-fat diets which overwhelm detoxification pathways or vitamin D deficiency are associated with increased levels of LCA. This in turn results in accumulation of toxic LCA with subsequent damage to the colonic epithelium and progression to cancer (35). Further, recent studies in mice demonstrated that activation of Vdr with vitamin D_3 stimulates the metabolic excretion of CDCA and not LCA, suggesting that Vdr is important for the regulation of CDCA levels (36). Consistent with these latest findings, we detected an increased serum concentration of CDCA, and not LCA or derivatives, in KO+DEN+Hh mice relative to WT+DEN+Hh and WT mice. Our data indicates that in KO+DEN+Hh mice, *Vdr* may have been induced by either CDCA and/or infection with Hh. TLR2 recognizes Hh and its signaling is important for Vdr expression (37,38). In the absence of CAR, Vdr activation may represent a compensatory response to increase metabolism and elimination of toxic compounds.

We also investigated the possible role of cathelicidin in tumor promotion. In human biliary epithelial cells, CDCA and UDCA regulate the expression of CAMP, the orthologue of mouse Camp, through FXR and VDR, respectively (39). Consistent with a mechanism involving nuclear receptors, we detected, relative to WT mice, significantly increased hepatic expression of *Vdr*, FXR, and *Camp* as well as increased concentration of serum CDCA during tumor promotion in KO mice treated with DEN and chronically infected with Hh. Upregulation of FXR in KO+DEN+Hh mice relative to WT mice may have been the result of increased serum concentration of TCA, another FXR agonist. In addition, immunohistochemistry detected CAMP mainly in neutrophils and macrophages in the livers of KO+DEN+Hh mice suggesting that this group of mice had an enhanced innate antimicrobial response against Hh. This finding may in part explain why tumor promotion in Hh-infected CAR deficient mice treated with DEN was also characterized by lower numbers of Hh in the liver compared to Hh-infected WT mice treated with DEN. Interestingly, increased CAMP expression has been detected in *H. pylori*-infected patients with gastritis and, when assessed by in vitro assays, CAMP was bactericidal for several *H. pylori* strains (40). Since a tumor promoting role of CAMP has been described in breast, lung, and ovarian cancer, our results also raise the possibility that this antimicrobial peptide may act as a tumor promoter in the liver during chronic infection with Hh (41).

Hepatitis in all Hh-infected mice indicated that inflammation was partially associated with tumor promotion. Increased hepatic expression of *Tlr2* and *Tnfα* correlated with Hh infection and induction of hepatitis. The role of Tnfα has been confirmed in Hh-induced intestinal tumor promotion (42,11) Promotion of liver dyplasia during Hh infection is associated with hepatic upregulation of *Tnfα*, *Il6*, and *Rela* (43). *Helicobacter* sp. infection did not appear to affect the colon or the small intestinal inflammation observed in PXR KO mice with upregulated NF-κB target genes; however, histological assessment of the livers was not documented (44). Increased proinflammatory gene expression in PXR KO mice was likely due to the loss of repression of NF-κB by PXR in vivo (44). Similarly, the upregulation of *Il6* and *Rela* in CAR KO mice relative to WT mice suggested that CAR also represses NF-κB activation and target genes such as *Il6*. Upregulation of beta-catenin in KO +DEN+Hh mice suggested a role of the Wnt signaling pathway in cell growth and differentiation during microbial liver tumor promotion.

Loss of metabolic detoxification has been proposed as a mechanism contributing to the pathophysiology of ulcerative colitis and PXR polymorphisms may influence survival in human cholestatic liver disease such as primary sclerosing cholangitis (45,46). Dual infection with *H. bilis* and *H. hepaticus* resulted in colitis that progressed to dysplasia in mice deficient in multidrug resistant protein 1a (Mdr1a or Abcb1a) gene which codes P-

glycoprotein, a membrane efflux pump expressed in intestinal epithelial cells that is regulated by CAR and PXR (47,2). Our study evaluating the effect of chronic *Helicobacter hepaticus* infection and inflammation in CAR deficient mice highlights how specific metabolic deficiencies impact liver tumor promotion through the accumulation of potentially toxic and carcinogenic endogenous compounds coupled with a persistent enterohepatic infection. Our findings demonstrate interplay between nuclear receptors, gastrointestinal microflora, and microbial-mediated immune responses that could be targeted as intervention strategy to prevent liver cancer progression. Our results also suggest that drugs that inhibit CAR may increase the risk of liver cancer in individuals infected with enterohepatic *Helicobacter* species. Interestingly, FXR, PXR, and CAR protect against hepatic bile acid toxicity in a complementary manner and nuclear receptors can be modulated by synthetic drugs and natural products (48,49). Further studies are needed in order to characterize how members of the gastrointestinal microflora modulate metabolism and impact carcinogenesis in mouse models of nuclear receptor deficiency as well as in nuclear receptor humanized mouse models.

Supplementary Material

Refer to Web version on PubMed Central for supplementary material.

Acknowledgments

The authors thank Agilent Technologies for access to the ESI-tandem-quadrupole mass spectrometer and Julie Marr of Agilent Technologies for helpful discussions. The authors also thank Elaine Robbins for assistance with preparation of the figures for publication. This study was supported by National Institutes of Health grants R01CA067529, R01DK052413, T32RR007036, P30ES002109, and P01CA026731.

References

1. Lundin A, Bok CM, Aronsson L, et al. Gut flora, Toll-like receptors and nuclear receptors: a tripartite communication that tunes innate immunity in large intestine. Cell Microbiol. 2008; 10:1093–103. [PubMed: 18088401]
2. Reschly EJ, Krasowski MD. Evolution and function of the NR1I nuclear hormone receptor subfamily (VDR, PXR, and CAR) with respect to metabolism of xenobiotics and endogenous compounds. Curr Drug Metab. 2006; 7:349–65. [PubMed: 16724925]
3. Bernstein H, Bernstein C, Payne CM, Dvorak K. Bile acids as endogenous etiologic agents in gastrointestinal cancer. World J Gastroenterol. 2009; 15:3329–40. [PubMed: 19610133]
4. Jansen PL. Endogenous bile acids as carcinogens. J Hepatol. 2007; 47:434–5. [PubMed: 17624466]
5. McGarr SE, Ridlon JM, Hylemon PB. Diet, anaerobic bacterial metabolism, and colon cancer: a review of the literature. J Clin Gastroenterol. 2005; 39:98–109. [PubMed: 15681903]
6. Huang W, Zhang J, Washington M, et al. Xenobiotic stress induces hepatomegaly and liver tumors via the nuclear receptor constitutive androstane receptor. Mol Endocrinol. 2005; 19:1646–53. [PubMed: 15831521]
7. Yamamoto Y, Moore R, Goldsworthy TL, Negishi M, Maronpot RR. The orphan nuclear receptor constitutive active/androstane receptor is essential for liver tumor promotion by phenobarbital in mice. Cancer Res. 2004; 64:7197–200. [PubMed: 15492232]
8. Diwan BA, Ward JM, Ramljak D, Anderson LM. Promotion by *Helicobacter hepaticus*-induced hepatitis of hepatic tumors initiated by N-nitrosodimethylamine in male A/JCr mice. Toxicol Pathol. 1997; 25:597–605. [PubMed: 9437805]
9. Fox JG, Feng Y, Theve EJ, et al. Gut microbes define liver cancer risk in mice exposed to chemical and viral transgenic hepatocarcinogens. Gut. 2010; 59:88–97. [PubMed: 19850960]
10. Nagamine CM, Rogers AB, Fox JG, Schauer DB. *Helicobacter hepaticus* promotes azoxymethane-initiated colon tumorigenesis in BALB/c-IL10-deficient mice. Int J Cancer. 2008; 122:832–8. [PubMed: 17957786]

11. Rao VP, Poutahidis T, Ge Z, et al. Innate immune inflammatory response against enteric bacteria *Helicobacter hepaticus* induces mammary adenocarcinoma in mice. Cancer Res. 2006; 66:7395–400. [PubMed: 16885333]
12. Maurer KJ, Carey MC, Fox JG. Roles of infection, inflammation, and the immune system in cholesterol gallstone formation. Gastroenterology. 2009; 136:425–40. [PubMed: 19109959]
13. García A, Ihrig MM, Fry RC, et al. Genetic susceptibility to chronic hepatitis is inherited codominantly in *Helicobacter hepaticus*-infected AB6F1 and B6AF1 hybrid male mice, and progression to hepatocellular carcinoma is linked to hepatic expression of lipogenic genes and immune function-associated networks. Infect Immun. 2008; 76:1866–76. [PubMed: 18285497]
14. Carter JH, Carter HW, Deddens JA, Hurst BM, George MH, DeAngelo AB. A 2-year dose-response study of lesion sequences during hepatocellular carcinogenesis in the male B6C3F(1) mouse given the drinking water chemical dichloroacetic acid. Environ Health Perspect. 2003; 111:53–64. [PubMed: 12515679]
15. Rogers AB, Theve EJ, Feng Y, et al. Hepatocellular carcinoma associated with liver-gender disruption in male mice. Cancer Res. 2007; 67:11536–46. [PubMed: 18089782]
16. Ge Z, White DA, Whary MT, Fox JG. Fluorogenic PCR-based quantitative detection of a murine pathogen, *Helicobacter hepaticus*. J Clin Microbiol. 2001; 39:2598–602. [PubMed: 11427576]
17. Takahashi M, Dinse GE, Foley JF, Hardisty JF, Maronpot RR. Comparative prevalence, multiplicity, and progression of spontaneous and vinyl carbamate-induced liver lesions in five strains of male mice. Toxicol Pathol. 2002; 30:599–605. [PubMed: 12371669]
18. Beilke LD, Aleksunes LM, Holland RD, et al. Constitutive androstane receptor-mediated changes in bile acid composition contributes to hepatoprotection from lithocholic acid-induced liver injury in mice. Drug Metab Dispos. 2009; 37:1035–45. [PubMed: 19196849]
19. Wagner M, Halilbasic E, Marschall HU, et al. CAR and PXR agonists stimulate hepatic bile acid and bilirubin detoxification and elimination pathways in mice. Hepatology. 2005; 42:420–30. [PubMed: 15986414]
20. Wei P, Zhang J, Dowhan DH, Han Y, Moore DD. Specific and overlapping functions of the nuclear hormone receptors CAR and PXR in xenobiotic response. Pharmacogenomics J. 2002; 2:117–26. [PubMed: 12049174]
21. Kim I, Morimura K, Shah Y, Yang Q, Ward JM, Gonzalez FJ. Spontaneous hepatocarcinogenesis in farnesoid X receptor-null mice. Carcinogenesis. 2007; 28:940–6. [PubMed: 17183066]
22. Maran RR, Thomas A, Roth M, et al. Farnesoid X receptor deficiency in mice leads to increased intestinal epithelial cell proliferation and tumor development. J Pharmacol Exp Ther. 2009; 328:469–77. [PubMed: 18981289]
23. Modica S, Murzilli S, Salvatore L, Schmidt DR, Moschetta A. Nuclear bile acid receptor FXR protects against intestinal tumorigenesis. Cancer Res. 2008; 68:9589–94. [PubMed: 19047134]
24. Yang F, Huang X, Yi T, Yen Y, Moore DD, Huang W. Spontaneous development of liver tumors in the absence of the bile acid receptor farnesoid X receptor. Cancer Res. 2007; 67:863–7. [PubMed: 17283114]
25. Blair PC, Popp JA, Bryant-Varela BJ, Thompson MB. Promotion of hepatocellular foci in female rats by chenodeoxycholic acid. Carcinogenesis. 1991; 12:59–63. [PubMed: 1988183]
26. Mahmoud NN, Dannenberg AJ, Bilinski RT, et al. Administration of an unconjugated bile acid increases duodenal tumors in a murine model of familial adenomatous polyposis. Carcinogenesis. 1999; 20:299–303. [PubMed: 10069468]
27. Reddy BS, Watanabe K, Weisburger JH, Wynder EL. Promoting effect of bile acids in colon carcinogenesis in germ-free and conventional F344 rats. Cancer Res. 1977; 37:3238–42. [PubMed: 884672]
28. Changbumrung S, Tungtrongchitr R, Migasena P, Chamroenngan S. Serum unconjugated primary and secondary bile acids in patients with cholangiocarcinoma and hepatocellular carcinoma. J Med Assoc Thai. 1990; 73:81–90. [PubMed: 2161896]
29. Fukase K, Ohtsuka H, Onogawa T, et al. Bile acids repress E-cadherin through the induction of Snail and increase cancer invasiveness in human hepatobiliary carcinoma. Cancer Sci. 2008; 99:1785–92. [PubMed: 18691339]

30. Araya Z, Wikvall K. 6alpha-hydroxylation of taurochenodeoxycholic acid and lithocholic acid by CYP3A4 in human liver microsomes. Biochim Biophys Acta. 1999; 1438:47–54. [PubMed: 10216279]
31. Hirano S, Masuda N. Enhancement of the 7 alpha-dehydroxylase activity of a gram-positive intestinal anaerobe by *Bacteroides* and its significance in the 7-dehydroxylation of ursodeoxycholic acid. J Lipid Res. 1982; 23:1152–8. [PubMed: 6960114]
32. Ge Z, Feng Y, Taylor NS, et al. Colonization dynamics of altered Schaedler flora is influenced by gender, aging, and *Helicobacter hepaticus* infection in the intestines of Swiss Webster mice. Appl Environ Microbiol. 2006; 72:5100–3. [PubMed: 16820515]
33. Kuehl CJ, Wood HD, Marsh TL, Schmidt TM, Young VB. Colonization of the cecal mucosa by *Helicobacter hepaticus* impacts the diversity of the indigenous microbiota. Infect Immun. 2005; 73:6952–61. [PubMed: 16177375]
34. Miyaguchi S, Watanabe T. The role of vitamin D3 receptor mRNA in the proliferation of hepatocellular carcinoma. Hepatogastroenterology. 2000; 47:468–72. [PubMed: 10791215]
35. Makishima M, Lu TT, Xie W, et al. Vitamin D receptor as an intestinal bile acid sensor. Science. 2002; 296:1313–6. [PubMed: 12016314]
36. Nishida S, Ozeki J, Makishima M. Modulation of bile acid metabolism by 1alpha-hydroxyvitamin D3 administration in mice. Drug Metab Dispos. 2009; 37:2037–44. [PubMed: 19581390]
37. Liu PT, Stenger S, Li H, et al. Toll-like receptor triggering of a vitamin D-mediated human antimicrobial response. Science. 2006; 311:1770–3. [PubMed: 16497887]
38. Mandell L, Moran AP, Cocchiarella A, et al. Intact gram-negative *Helicobacter pylori*, *Helicobacter felis*, and *Helicobacter hepaticus* bacteria activate innate immunity via toll-like receptor 2 but not toll-like receptor 4. Infect Immun. 2004; 72:6446–54. [PubMed: 15501775]
39. D'Aldebert E, Biyeyeme Bi Mve MJ, Mergey M, et al. Bile salts control the antimicrobial peptide cathelicidin through nuclear receptors in the human biliary epithelium. Gastroenterology. 2009; 136:1435–43. [PubMed: 19245866]
40. Hase K, Murakami M, Iimura M, et al. Expression of LL-37 by human gastric epithelial cells as a potential host defense mechanism against *Helicobacter pylori*. Gastroenterology. 2003; 125:1613–25. [PubMed: 14724813]
41. Coffelt SB, Marini FC, Watson K, et al. The pro-inflammatory peptide LL-37 promotes ovarian tumor progression through recruitment of multipotent mesenchymal stromal cells. Proc Natl Acad Sci U S A. 2009; 106:3806–11. [PubMed: 19234121]
42. Erdman SE, Rao VP, Poutahidis T, et al. Nitric oxide and TNF-alpha trigger colonic inflammation and carcinogenesis in *Helicobacter hepaticus*-infected, Rag2-deficient mice. Proc Natl Acad Sci U S A. 2009; 106:1027–32. [PubMed: 19164562]
43. Ge Z, Rogers AB, Feng Y, et al. Bacterial cytolethal distending toxin promotes the development of dysplasia in a model of microbially induced hepatocarcinogenesis. Cell Microbiol. 2007; 9:2070–80. [PubMed: 17441986]
44. Zhou C, Tabb MM, Nelson EL, et al. Mutual repression between steroid and xenobiotic receptor and NF-kappaB signaling pathways links xenobiotic metabolism and inflammation. J Clin Invest. 2006; 116:2280–9. [PubMed: 16841097]
45. Karlsen TH, Lie BA, Frey Froslie K, et al. Polymorphisms in the steroid and xenobiotic receptor gene influence survival in primary sclerosing cholangitis. Gastroenterology. 2006; 131:781–7. [PubMed: 16952547]
46. Langmann T, Moehle C, Mauerer R, et al. Loss of detoxification in inflammatory bowel disease: dysregulation of pregnane X receptor target genes. Gastroenterology. 2004; 127:26–40. [PubMed: 15236169]
47. Maggio-Price L, Bielefeldt-Ohmann H, Treuting P, et al. Dual infection with *Helicobacter bilis* and *Helicobacter hepaticus* in p-glycoprotein-deficient *mdr1a*-/- mice results in colitis that progresses to dysplasia. Am J Pathol. 2005; 166:1793–806. [PubMed: 15920164]
48. Chang TK, Waxman DJ. Synthetic drugs and natural products as modulators of constitutive androstane receptor (CAR) and pregnane X receptor (PXR). Drug Metab Rev. 2006; 38:51–73. [PubMed: 16684648]

49. Guo GL, Lambert G, Negishi M, et al. Complementary roles of farnesoid X receptor, pregnane X receptor, and constitutive androstane receptor in protection against bile acid toxicity. J Biol Chem. 2003; 278:45062–71. [PubMed: 12923173]

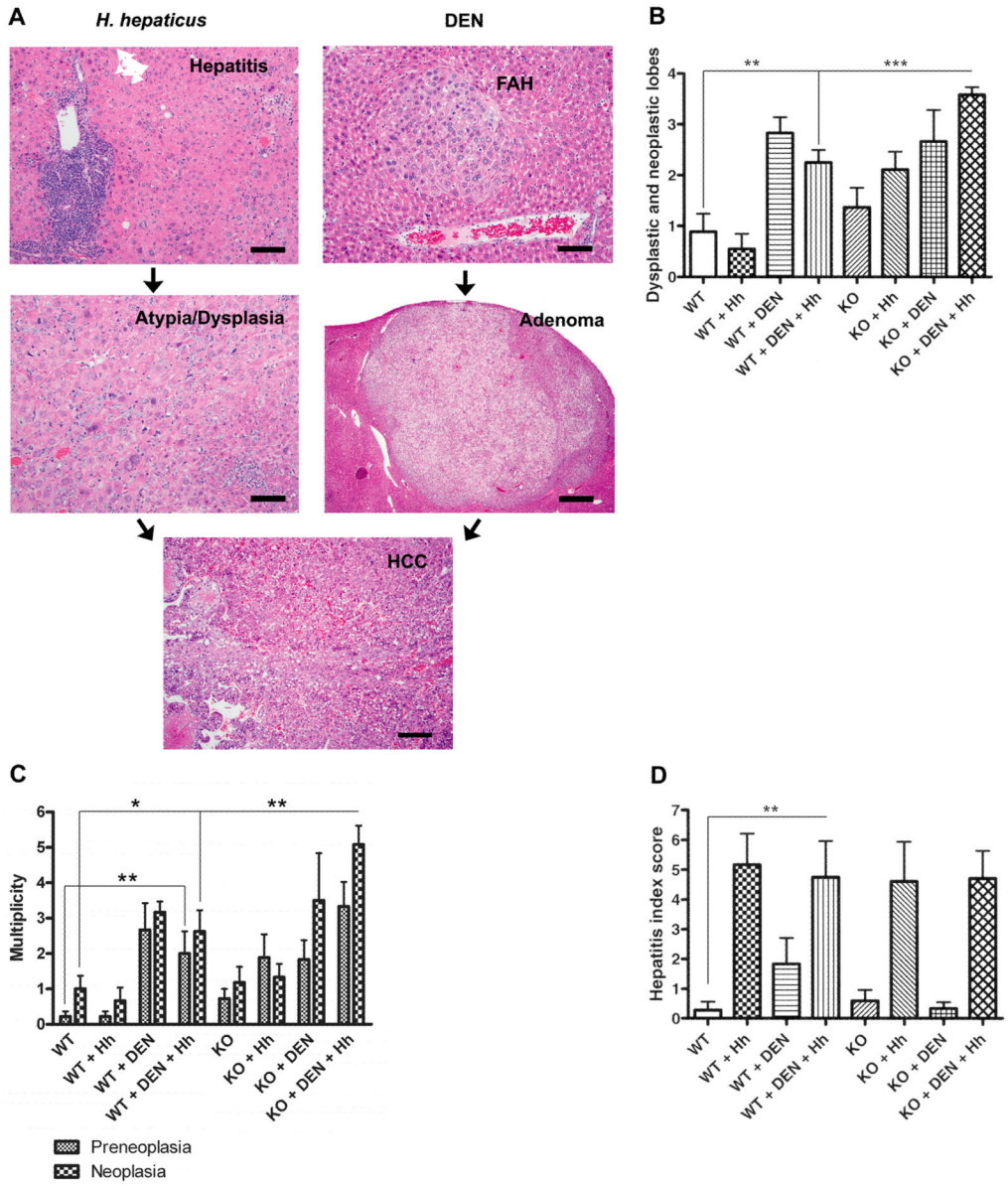

Fig. 1.

A, Representative microscopic liver lesions observed in this study and the schematic possible tumor progression in various groups: FAH (bar=100 μm), adenoma (HCA) with clear cell/vacuolated changes (bar=400 μm), and HCC (bar=200 μm). The HCC was solid to trabecular with multifocal necrosis. Hh infection with concomitant hepatitis (bar=40 μm) may also progress to non-discrete areas of dysplasia (bar=40 μm) and subsequently to HCC (hematoxylin and eosin). Alternatively, Hh infection can induce FAH, HCA, and HCC. DEN, diethylnitrosamine. B, Number of dysplastic and neoplastic liver lobes per group. The number of dysplastic and neoplastic liver lobes was found to be significantly different in other comparisons. For example: WT vs. WT+DEN ($P<0.002$); WT vs. KO+DEN ($P<0.02$); WT+Hh vs. KO+Hh mice ($P<0.004$). C, Multiplicity of preneoplasia (FAH and LFCA combined) and neoplasia (HCA and HCC combined) per group. The multiplicity of preneoplasia was found to be significantly different in other comparisons. For example: WT vs. WT+DEN ($P<0.002$); WT+Hh vs. KO+Hh ($P<0.02$); WT vs. KO+DEN+Hh ($P<0.001$).

The multiplicity of neoplasia was found to be significantly different in other comparisons. For example: WT vs. WT+DEN ($P<0.001$); WT+Hh vs. WT+DEN+Hh ($P<0.01$); WT vs. KO+DEN+Hh ($P<0.0001$). D, All groups of Hh-infected mice developed comparably high HI scores. *, $P\leq0.05$; **, $P\leq0.01$; ***, $P\leq0.001$.

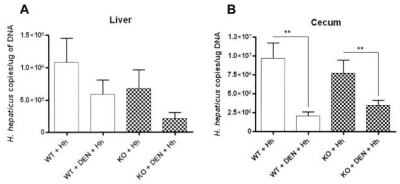

Fig. 2.

A and B, *H. hepaticus* colonization in the liver and cecum as determined by real-time quantitative PCR. **, P≤0.01.

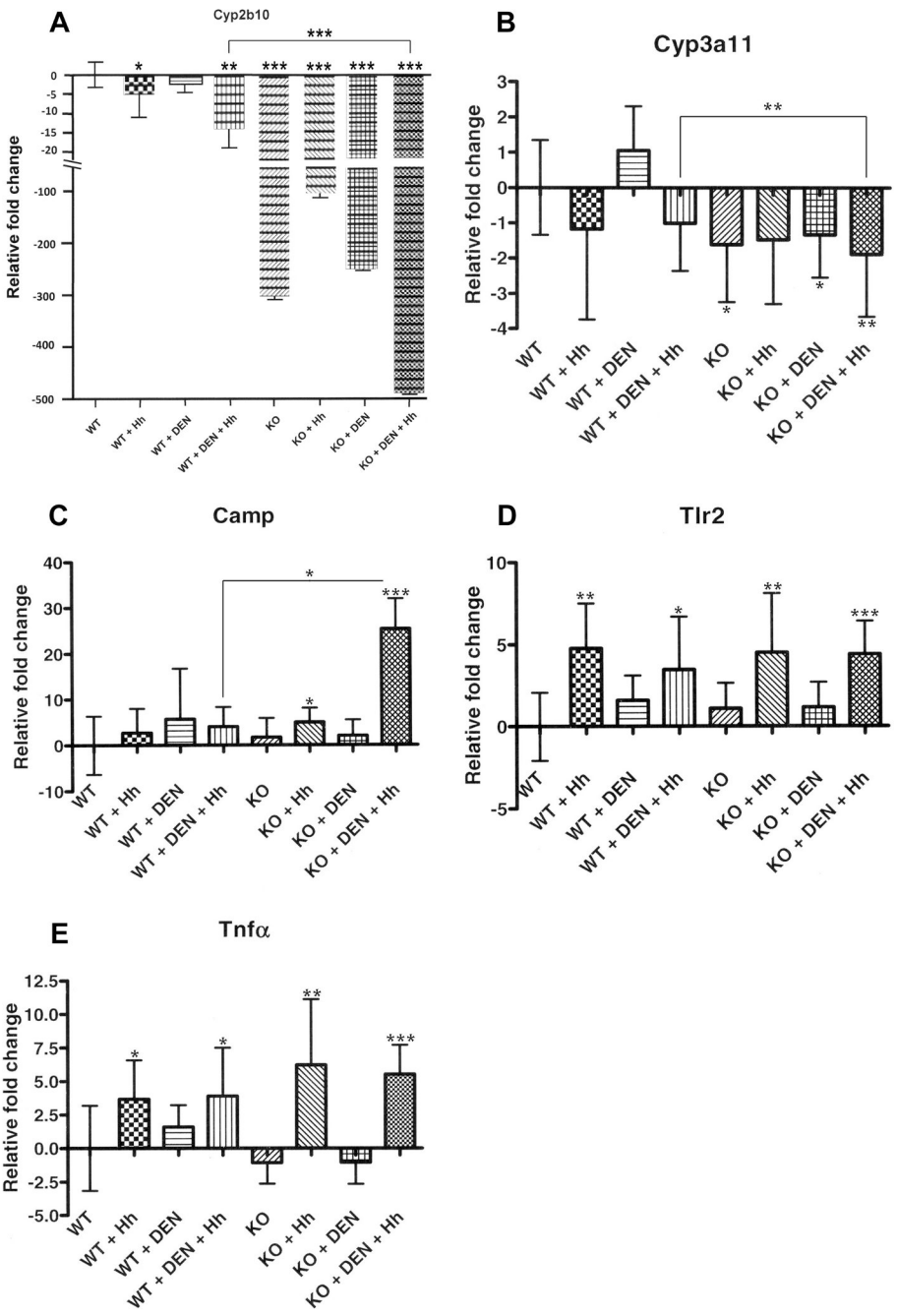

Fig. 3.

Gene expression analyses using real-time quantitative PCR. A, Cytochrome P450, family 2, subfamily b, polypeptide 10 (*Cyp2b10*). B, Cytochrome P450, family 3, subfamily a, polypeptide 11 (*Cyp3a11*). C, Cathelicidin antimicrobial peptide (*Camp*). D, Toll-like receptor 2 (*Tlr2*). E, Tumor necrosis factor (*Tnfα*). *, P≤0.05; **, P≤0.01. ***, P≤0.001.

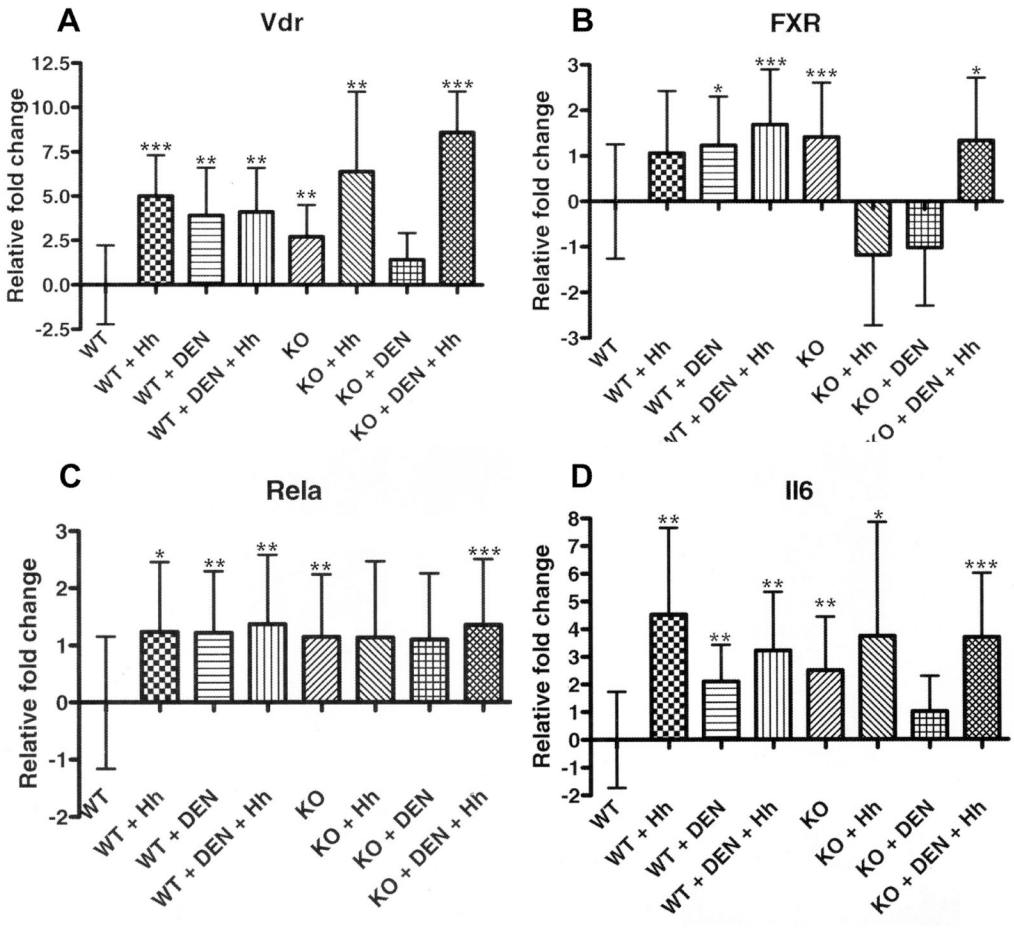

Fig. 4.

Gene expression analyses using real-time quantitative PCR. A, Vitamin D receptor (*Vdr*). B, Farsenoid X receptor (FXR). C, p65 (*Rela*). D, Interleukin 6 (*Il6*). *, P≤0.05; **, P≤0.01. ***, P≤0.001.

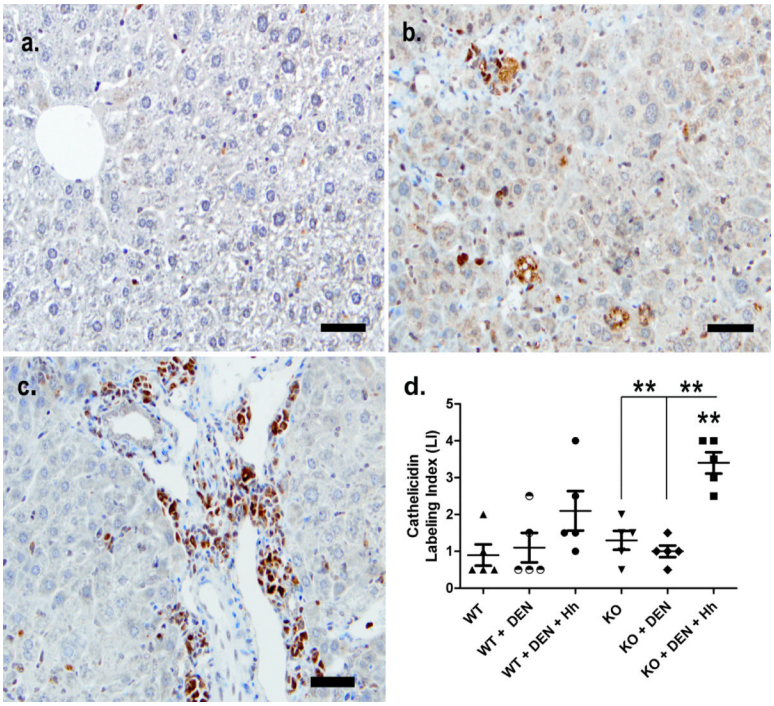

Fig. 5.

Immunohistochemical detection of cathelicidin antimicrobial peptide in the livers of KO +DEN+Hh mice (within lobule, B; portal region, C) compared to WT mice (uninfected and without diethylnitrosamine) (centrilobular area, A) (bar=100 μm). D, Cathelicidin Labeling Index (LI) of epithelial and inflammatory cells in the liver. **, P≤0.01.

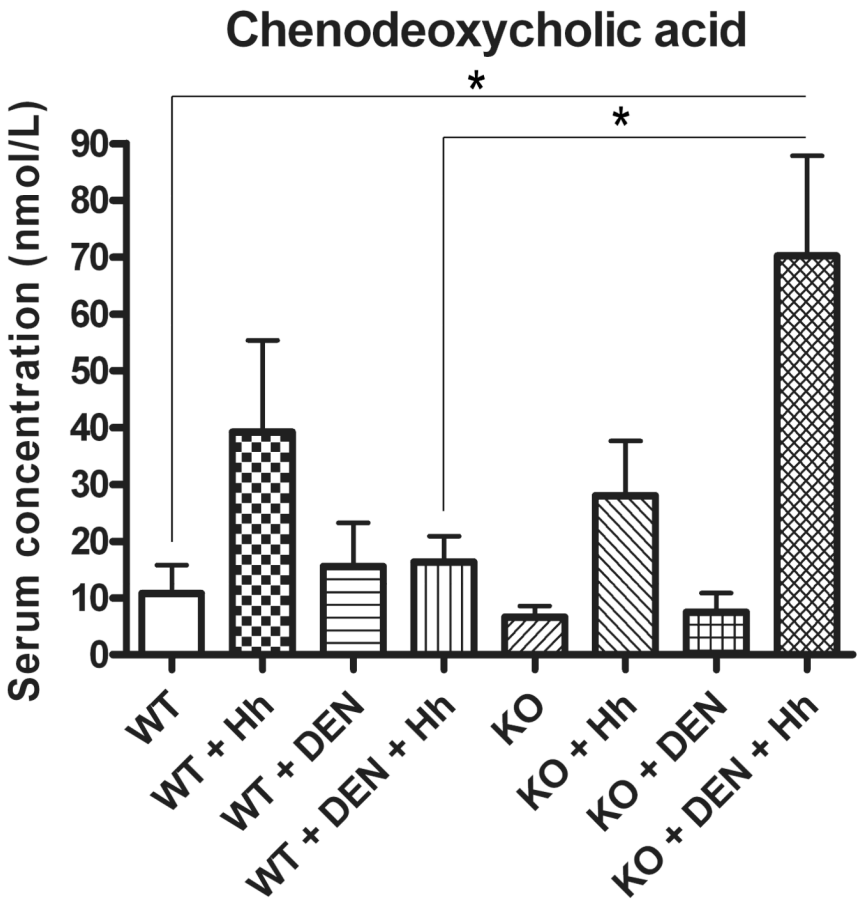

Fig. 6.

Serum concentration of the dihydroxylated primary bile acid chenodeoxycholic acid (CDCA) as measured by LC-MS/MS. *, P≤0.05.

Table 1
Groups and numbers of mice in this study*

Genotype	Tumor initiation (DEN‡)	Tumor promotion (Infection)	Number of mice§	Group designation
$CAR^{+/+}$	No	No	10 (9)	WT
$CAR^{+/+}$	No	Yes	10 (9)	WT+Hh
$CAR^{+/+}$	Yes	No	10 (6)†	WT+DEN
$CAR^{+/+}$	Yes	Yes	13 (8)†	WT+DEN+Hh
$CAR^{-/-}$	No	No	12 (11)	KO
$CAR^{-/-}$	No	Yes	9 (9)	KO+Hh
$CAR^{-/-}$	Yes	No	9 (6)	KO+DEN
$CAR^{-/-}$	Yes	Yes	13 (12)	KO+DEN+Hh

*The number of animals evaluated per group for histopathology, gene expression analyses, and bile acid determination. Serum from one animal in the WT group was not available for bile acid determination.

‡DEN, diethylnitrosamine.

§Numbers in parentheses indicate the number of mice that were evaluated at the end of the study (~50 weeks postinoculation).

†Three mice in each group were euthanized at ~30 weeks postinoculation to evaluate the liver.